research paper

JOURNAL OF APPLIED CRYSTALLOGRAPHY

ISSN 1600-5767

Characterization of ammonium dihydrogen phosphate crystals for soft X-ray optics of the Beam Expander Testing X-ray facility (BEaTriX)

Claudio Ferrari,[a]* Sara Beretta,[a] Bianca Salmaso,[b] Giovanni Pareschi,[b] Gianpiero Tagliaferri,[b] Stefano Basso,[b] Daniele Spiga,[b] Carlo Pelliciari[c] and Enrico Giro[b]

[a]IMEM-CNR Insitute, parco Area delle Scienze 37/A, Parma, PR 43124, Italy, [b]INAF–Osservatorio Astronomico di Brera, via E. Bianchi 46, Merate, LC 23807, Italy, and [c]MPE–Department of High-Energy Astrophysics, Max Plank Insitute for Extraterrestrial Physics, Giessenbachstrasse 1, Garching bei München, 85748, Germany. *Correspondence e-mail: claudio.ferrari@imem.cnr.it

Received 31 January 2019
Accepted 4 April 2019

Edited by J. M. García-Ruiz, Instituto Andaluz de Ciencias de la Tierra, Granada, Spain

Keywords: X-ray astronomy; ammonium dihydrogen phosphate; ADP; crystalline perfection; X-ray topography; residual strain measurement; lattice plane curvature measurement.

A new type of X-ray facility, the Beam Expander Testing X-ray facility (BEaTriX), has been designed and is now under construction at INAF–Osservatorio Astronomico di Brera (Merate, Italy) to perform the acceptance tests of the silicon pore optics modules of the ATHENA X-ray telescope. Crystals of high perfection and large dimensions are needed in order to obtain a wide beam (20 × 6 cm) with an X-ray divergence of <0.5″ and an X-ray energy purity $\Delta E/E < 10^{-5}$. To generate X-ray diffracted beams at an X-ray energy of 1.49 keV, ammonium dihydrogen phosphate (ADP) crystals have been considered among other possible choices, because of their reported crystal quality and because they can be grown at sufficiently large size at a reasonable price. In the present paper, the results of the characterization of crystalline quality and lattice planarity of a 20 × 20 × 2 mm ADP sample are reported.

1. Introduction

ATHENA (Advanced Telescope for High Energy Astrophysics) is an ESA X-ray mission aimed at understanding the evolution of the universe and the key role of black holes. The 2.4 m diameter optics are composed of more than 700 mirror modules (MM) that need to be tested and accepted before integration. To this end, INAF–Osservatorio Astronomico di Brera started in 2012 to design a facility based on the generation of a broad, uniform and low-divergent X-ray beam to illuminate the full aperture of the ATHENA MM with a beam with vertical and horizontal divergence lower than 1.5″ half energy width (HEW) (Spiga *et al.*, 2012, 2014, 2016; Pelliciari *et al.*, 2015). The Beam Expander Testing X-ray facility (BEaTriX) is now under construction for the 4.51 keV energy, and it is built to host a second beamline at 1.49 keV. The two energies are required to accept the MM, by measuring their point spread function and effective area.

For each beamline, the design foresees an X-ray microfocus source, a paraboloidal mirror, a symmetrical channel cut crystal as monochromator and an asymmetrically cut crystal for beam expansion. The vertical divergence of the final beam is limited by the 30 µm dimension of the focal spot of the X-ray source, whereas the horizontal divergence is also defined by the X-ray monochromators and by the asymmetrically cut crystal for the beam expansion (Salmaso *et al.*, 2018). Four reflections on a monochromation system composed of symmetrically cut crystals are needed to reduce

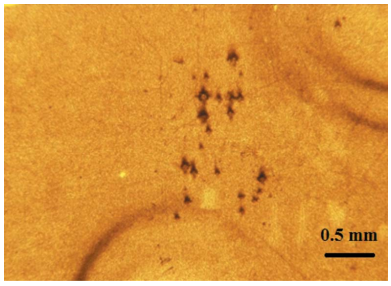

the bandwidth of the beam and limit the horizontal divergence, which is highly dependent on the energy-dispersive properties of the asymmetrically cut crystals (Sánchez del Río & Cerrina, 1992).

For the fulfillment of the projected optical quality of the final beam, the crystallographic quality of the monochromators and of the beam expander is fundamental: the presence of crystallographic defects and of lattice plane curvature can broaden the X-ray reflectivity profiles of the crystals. In the BEaTriX error budget tree, 0.5″ HEW have been allocated for deviation from ideality of the crystals. A simple calculation shows that, to maintain the horizontal divergence lower than 0.5″ along the 170 mm dimension of the expander crystal, the minimum acceptable curvature radius R of the reflecting planes is around 30 km.

For the 4.51 keV beamline (Ti $K\alpha$ line), the monochromators and the beam expander have been realized using extremely low doped, dislocation-free silicon crystals characterized by a very high perfection. The very low doping prevents the formation of residual strains in the material generated by non-uniform doping of the crystal during the crystal growth (Celotti *et al.*, 1974) and possible lattice bending.

The lower-energy beamline (1.49 keV , Al $K\alpha$ line), corresponding to a wavelength of 8.314 Å, is more challenging as crystals with large lattice spacing are needed, involving materials less known than the widely used silicon. In this wavelength range, the tetragonal ammonium dihydrogen phosphate (ADP) crystal is used for X-ray spectroscopy (https://www.crystals.saint-gobain.com/document/X-ray-monochromators), and it was also proposed in the past for X-ray astronomy (Burek *et al.*, 1974). The lattice spacing (a = b = 7.53, c = 7.742 Å) and structure permit the production of an intense (101) diffracted beam at $\theta_{\rm Bragg}$ = 51.417° for the Al $K\alpha$ wavelength. Another important parameter is the obtainable crystal dimension: the crystal producer confirmed the possibility to obtain a 5.1° offcut crystal with respect to the (001) planes with dimensions of up to 120 × 80 mm and suitable for use as a 50× beam expander for the 1.49 keV beam.

ADP crystals are usually grown in large dimensions from aqueous solution. They were proposed more than 30 years ago for nonlinear optical applications [see for instance Moritani *et al.* (1983)]. Their structural characterization, performed by X-ray topography, has confirmed that the crystals are characterized by high crystal perfection (Deslattes *et al.*, 1966; Bhagavannarayana *et al.*, 2006; Bhat *et al.*, 1983), nearly dislocation free and free of inclusions.

In order to assess if the commercially available ADP crystals can provide a crystal perfection compatible with the demanding requirements of the BEaTriX project, a detailed characterization is needed to check if they are free of dislocations and other structural defects, and if the lattice planes are as flat as required, without bending due to the presence of residual strains. The purpose of the present article is the evaluation of the ADP crystal quality, in view of its use in the BEaTriX project.

2. Experimental

A 20 × 20 × 2 mm ADP crystal, with the 20 × 20 mm face (001) oriented, was procured from Saint Gobain to perform preliminary analysis of its crystallographic quality. The ADP crystal has an orthorhombic cell with a = b = 7.53, c = 7.542 Å, and it is designed for X-ray spectroscopy using the (101) diffracting planes with spacing 5.324 Å, for diffraction in the range of soft X-rays. ADP crystals are usually grown from solution from seed crystals, and it is expected that the present sample is indicative of the quality of the whole ingot, even if the information on the sample position within the ingot is not available.

3. X-ray topography measurements

The X-ray topographic characterization has been performed by using a double-crystal topographic camera with a copper

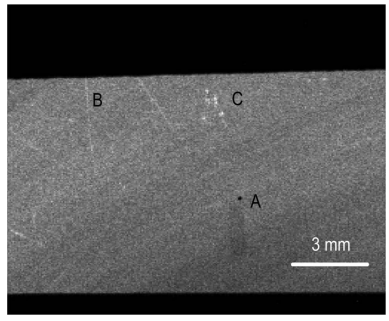

Figure 1
Double-crystal topograph of the ADP sample, registered using an Advacam MiniPIX camera, a Ge 620 monochromator and Cu $K\alpha_1$ radiation. A: defective pixel; B: tiny scratches due to handling or surface preparation; C: defects, possibly dislocations or crystal inclusions.

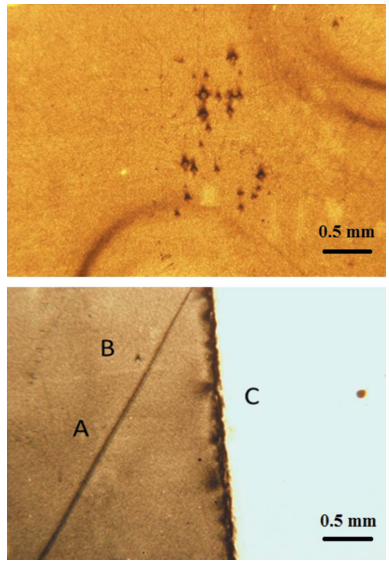

Figure 2
Double-crystal topographs of the ADP sample registered on nuclear emulsion using a Ge 620 monochromator and Cu $K\alpha_1$ radiation. The contrast is reversed with respect to Fig. 1. (*a*) 3 × 4 mm area showing a magnification of Fig. 1 with emerging dislocations or inclusions. (*b*) 3 × 4 mm area near the edge of the crystal, showing a scratch A, an emerging dislocation B and the contrast near the edge of the crystal C.

anode ($\lambda_{Cu\ K\alpha}$ = 1.54051 Å) and an asymmetrically cut Ge 620 perfect crystal as a monochromator with a Bragg angle of θ_B = 59.6° (Jenichen *et al.*, 1988). This is not far from the (008) Cu $K\alpha$ Bragg angle θ_B = 54.79° of ADP, thus reducing the effect of wavelength dispersion due to the difference between Bragg angles of the Ge monochromator and sample.

In the double-crystal topographic camera, the wide beam impinges on the sample and the topograph is obtained by registering the diffracted beam on a detector or on a film, while maintaining fixed the angle of incidence. For an overall evaluation of the crystal an Advacam MiniPIX camera, 256 × 256 pixels with a pitch of 55 µm, has been used to register the diffracted image, permitting us to reduce the exposure time to approximately half an hour. The topograph reported in Fig. 1 shows a uniform contrast with very few defects. Some of these defects are magnified in Figs. 2(*a*) and 2(*b*). These two images have been obtained by using topograph plates with an image resolution of a few micrometres but much longer exposure time. The image reported in Fig. 1 shows only the presence of a few surface scratches and some isolated point defects, presumably emerging dislocations or tiny inclusions.

In Fig. 2 the X-ray topographs show very few crystallographic defects, demonstrating the very high quality of the ADP crystal. The visible contrast near the edge of the crystal in Fig. 2(*b*) is clearly introduced by the cutting process. It is evident that the residual strain associated with the cutting process has not been removed by the etching or the polishing process and produces a characteristic strain contrast.

4. X-ray diffraction profile measurements

Measurement of the X-ray diffraction profile and the full width at half-maximum (FWHM) is considered a preliminary and effective test of the quality of the crystal, since the presence of defects always broadens the reflectivity profile. The theoretical diffraction profile, which corresponds to the perfect and strain-free crystal, is calculated by using the dynamical theory of X-ray diffraction. The calculation of the theoretical diffraction profile was obtained from the Stepanov X-ray server (http://x-server.gmca.aps.anl.gov/) of Argonne National Laboratory after including in the database the ADP crystal structure. The 004 theoretical diffraction profiles for σ polarization (electrical field perpendicular to the scattering plane) and π polarization for the Cu $K\alpha$ radiation are reported in Fig. 3. The FWHMs of the σ and π profiles are 0.56 and 0.34″, respectively.

From the simulations it is clear that a direct measurement of the reflectivity profile is very difficult owing to the need for a very parallel and monochromatic X-ray beam as a probe. An alternative method to verify the crystallographic quality of the sample is based on the measurement of the integrated intensity, that is the area of the reflectivity profile normalized by the incident beam intensity, a parameter almost independent of the divergence and wavelength purity of the X-ray source.

The integrated intensity is a parameter very sensitive to the crystal quality. It has a minimum value for a perfect crystal and increases rapidly with defect density by up to two orders of magnitude for ideally imperfect crystals (ideal mosaic) (Authier & Malgrange, 1998). The measurement was performed with a Panalytical X'Pert diffractometer using a four-crystal Ge 220 monochromator, with a Ge 220 Bragg angle of θ_B = 22.64°, not far from the 004 Cu $K\alpha$ Bragg angle θ_B = 24.112° of ADP, thus reducing the effect of wavelength dispersion. Note that the 'quality' of the crystal measured as a deviation from the results of the dynamical theory valid for perfect crystals is measured here by using a shorter wavelength than that intended for the application (λ = 1.54051 Å of Cu $K\alpha_1$ with respect to λ = 8.339 Å of Al $K\alpha_1$). On the other hand the deviation from the ideal crystal is itself dependent on the X-ray energy. In general by increasing the X-ray energy the integrated intensity may pass from the value corresponding to a perfect crystal to that of an ideal mosaic one. Examples of this are reported by Authier & Malgrange (1998), for Cu crystals of different perfection.

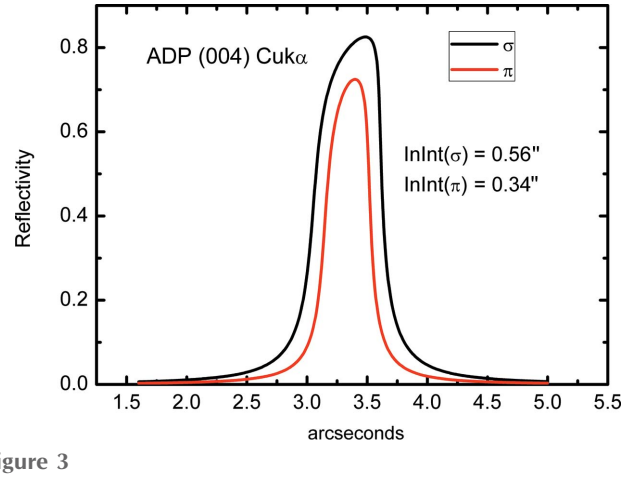

Figure 3
σ and π intrinsic diffraction profiles of ADP 004 at E = 8.04 keV X-ray beam energy as calculated by the Stepanov X-ray server (http://x-server.gmca.aps.anl.gov/) of Argonne National Laboratory. The x axis represents the deviation from nominal Bragg angle.

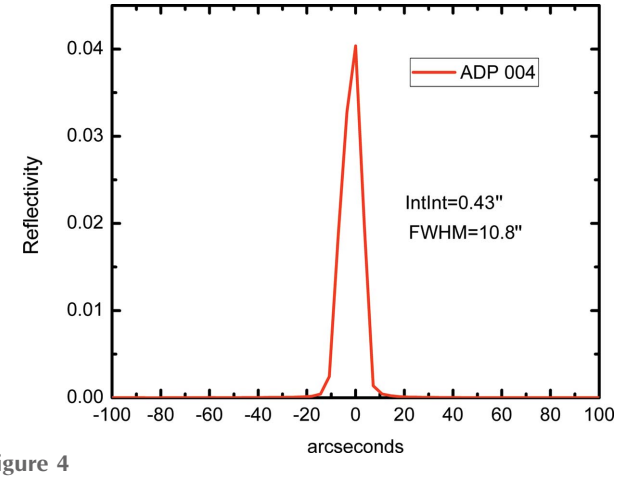

Figure 4
Experimental ADP 004 Cu $K\alpha$ diffraction profile measured with a Philips MRD diffractometer with a Bartels 4× Ge220 monochromator. The x axis is centered on the peak position.

For an accurate measurement it is necessary to take into account the polarization of the incident X-ray beam produced by the monochromator due to the four successive Ge 220 reflections. The polarization of the X-ray beam produced by the monochromator has been calculated by considering the σ and π profiles of each Ge 220 reflection. Owing to the four successive reflections the final profile of each component is calculated by taking the fourth power of the intrinsic σ and π profiles. The resulting profiles have integrated intensities of 8.246 and 4.837″, respectively. The exit beam is 63% σ and 37% π polarized, respectively. In this way the expected integrated intensity of the ADP 004 reflection profile is

$$\mathrm{IntInt}_{\mathrm{theor}} = \frac{8.246}{8.246 + 4.837} \times 0.56 + \frac{4.837}{8.246 + 4.837} \times 0.34 = 0.48''. \quad (1)$$

The ADP 004 experimental diffraction profile, normalized with the value of incident beam intensity, is reported in Fig. 4. As expected, the experimental FWHM is much larger than the value predicted by simulation, but the value of the integrated intensity is close (∼9% lower) to the value for a perfect crystal. Since any structural defect or residual strain leads to an increase of the integrated intensity, this demonstrates the excellent crystallographic quality of the sample and that the experimental FWHM is determined by the incident beam conditions. A possible explanation of the lower experimental integrated intensity with respect to the simulated is the lack of a Debye–Waller attenuation factor in the ADP database used for the calculation.

We conclude here that the analyzed ADP crystal behaves as a perfect crystal in terms of integrated intensity measurement for the Cu $K\alpha_1$ energy. According to X-ray diffraction theory, crystals which appear perfect at a given energy are necessarily perfect at lower energies. So we may conclude that the sample can be considered perfect also for Al $K\alpha_1$ X-rays as proposed for the BEaTriX application.

5. Curvature measurement

The second important parameter affecting the performance of the monochromator is the presence of curvature in the crystal. From the allocated error of 0.5″, a crystal of 120 mm length has a minimum acceptable curvature radius of the order R = 25 km. The curvature of the sample was obtained by measuring the shift of the Bragg peak position as a function of the position of the X-ray beam on the sample (Fig. 5). The Bragg peak shift $\delta\theta$ is related to the curvature R by $R = x/\delta\theta$, x being the distance between the two points of the measurement (Buffagni *et al.*, 2012). A linear dependence of the peak position shift as a function of position is an indication of a uniform curvature. In the geometry of our diffractometer, a peak position shift to higher angles with increasing x is an indication of a concave curvature.

To perform this measurement with the required accuracy, the translation stage of the crystal holder must be very reliable: for this purpose the stage of the diffractometer (Philips MRD) is based on the translation of the sample holder on a rectified surface. The system has been tested on a perfect silicon 2 mm-thick sample. Cu $K\alpha$ 004 reflectivity profiles taken with 5 mm spacing on the front and rear surface of a flat silicon wafer are reported in Fig. 6.

The peak position shifts, measured on both sides of the silicon wafer, are reported in Fig. 6(*b*). In both cases the Bragg peak positions decrease as x increases. This demonstrates that the calculated curvature is apparent and that the shifts are due to the mechanical inaccuracy of the translation stage. By repeating the measurements on the same side, nearly identical results are obtained.

Similar measurements have been performed on the 20 × 20 × 2 mm ADP sample using the ADP 004 reflection. The experimental curves are reported in Fig. 7(*a*) and the shift of the Bragg peak as a function of the position in Fig. 7(*b*). The peak position shifts reported in Fig. 7(*b*) are compensated by the mechanical inaccuracy of the translation stage determined in the previous step. In this way an R = 1350 m concave curvature is obtained, a value much smaller than the required value of 25 km.

The most reasonable explanation of the curvature is the presence of residual strain associated with the unpolished side of the sample. The surface damage introduces a local compressive strain and produces a curvature of the sample that is convex on the damaged side (Ferrari *et al.*, 2013) and concave on the opposite side, as in the present case. This

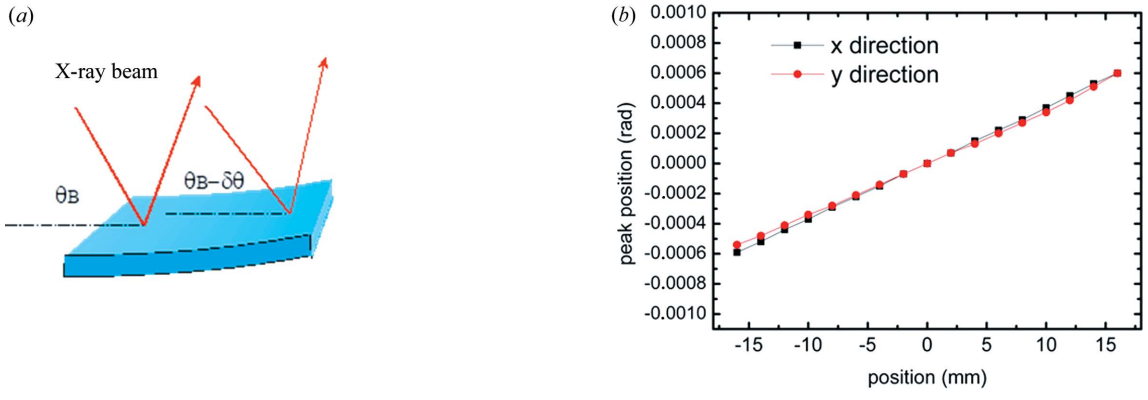

Figure 5
(*a*) Method of curvature measurement in large crystals. (*b*) Measurement of curvature in a spherically bent crystal with radius of curvature R = 27 m.

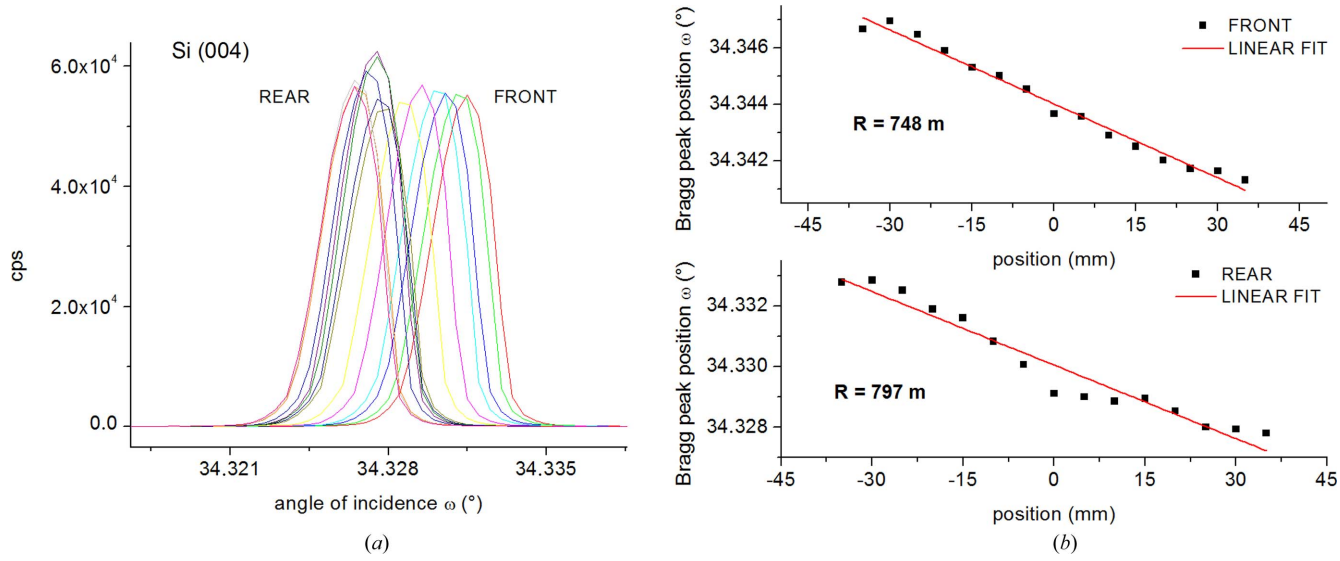

Figure 6
(*a*) 004 reflectivity profiles taken on both sides of the wafer, with 5 mm spacing between adjacent points in a 70 mm range in a 2 mm-thick perfect silicon crystal. (*b*) Bragg angle shifts measured on the front and rear surface. The apparent radius of curvature is reported.

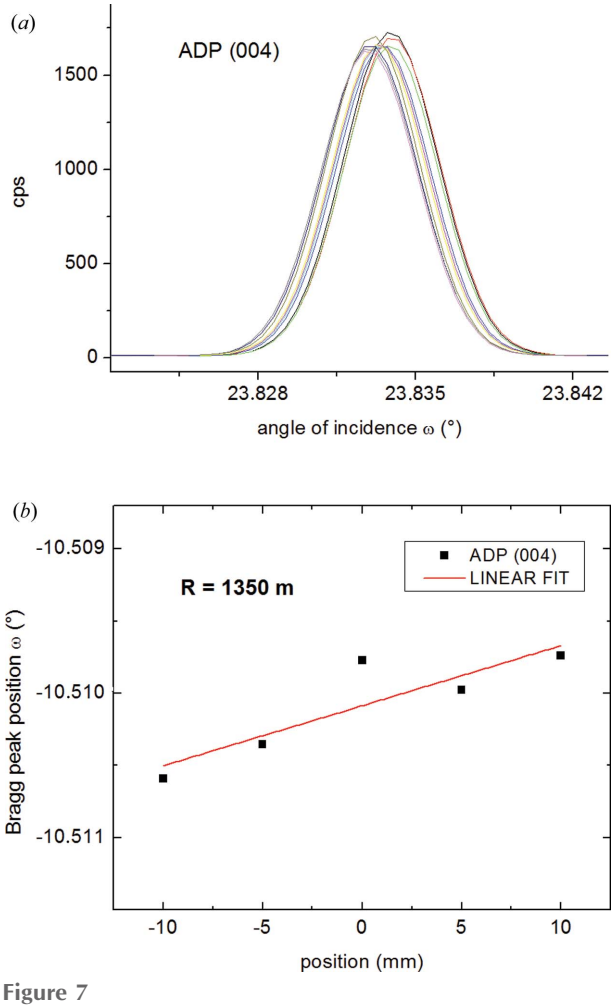

Figure 7
(*a*) ADP 004 reflectivity profiles spaced 2 mm between adjacent points in a 20 mm range. (*b*) Bragg peak angular position shift in a 20 mm range of the ADP 004 reflectivity profiles.

hypothesis is confirmed by the presence of strain at the edges of the crystal, as observed in the topograph of Fig. 2(*b*). New measurements on a double-sided ADP sample are planned, to fully validate this hypothesis.

For the application in the BEaTriX facility, a beam expander crystal thicker than 2 mm (the thickness of the present sample) will be considered, in order to increase the rigidity of the piece. If the resulting beam expander has a curvature above specifications, possible recovery actions will include the use of a bending system to compensate for the residual curvature.

6. Conclusion

ADP organic crystals have been considered to realize the monochromator and beam expander of the 1.49 keV beamline of the BEaTriX facility, designed to test the silicon pore optics modules of the ATHENA X-ray telescope. For this application it is of fundamental importance that the crystals are free of structural defects, such as dislocations and inclusions, and the lattice planes are perfectly flat. To assess the possible use of ADP for this application, we have characterized a 20 × 20 × 2 mm ADP commercial sample by X-ray topography and reflectivity profile measurements.

From the point of view of the crystallographic quality, an X-ray topograph showed very few dislocations and surface scratches, almost compatible with the proposed application. Moreover, accurate measurements of the integrated intensity of the Cu $K\alpha$ 004 reflectivity profile gave results in line with those expected for a perfect crystal. Of course, the sample analyzed has a quite limited area with respect to the area of the projected Al $K\alpha$ beam expander crystal, so these results may not be completely applicable to a larger crystal, but they do give an indication of the expected crystal quality.

The lattice curvature measured with the method of Bragg peak position variation as a function of the position showed a curvature of the sample of R = 1350 m, much smaller than the acceptable bending radius of lattice planes for the BEaTriX facility. Further tests on a double-side-polished ADP sample are planned to check if the curvature is due to the residual stress of the second unpolished side in the present sample. A final recovery action is defined in any case, which foresees the application of an elastic bending to the crystal to compensate the spontaneous curvature.

Acknowledgements

The authors are grateful to Dr Ivo Ferreira and Dr Marcos Bavdaz for reporting the BEaTriX project results to ESA and scientific support.

Funding information

The study of BEaTriX started in 2012 supported by the AHEAD H2020 project and also supported by an ESA contract.

References

Authier, A. & Malgrange, C. (1998). *Acta Cryst.* A**54**, 806–819.
Bhagavannarayana, G., Parthiban, S. & Meenakshisundaram, S. (2006). *J. Appl. Cryst.* **39**, 784–790.
Bhat, H. L., Roberts, K. J. & Sherwood, J. N. (1983). *J. Appl. Cryst.* **16**, 390–398.
Buffagni, E., Ferrari, C., Rossi, F., Marchini, L. & Zappettini, A. (2012). *Opt. Eng.* **51**, 056501.
Burek, A. J., Barrus, D. M. & Blake, R. L. (1974). *ApJ*, **191**, 533–544.
Celotti, G., Nobili, D. & Ostoja, P. (1974). *J. Mater. Sci.* **9**, 821–828.
Deslattes, R. D., Torgesen, J. L., Paretzkin, B. & Horton, A. T. (1966). *J. Appl. Phys.* **37**, 541–548.
Ferrari, C., Buffagni, E., Bonnini, E. & Korytar, D. (2013). *J. Appl. Cryst.* **46**, 1576–1581.
Jenichen, B., Kohler, R. & Mohling, W. (1988). *J. Phys. E Sci. Instrum.* **21**, 1062–1066.
Moritani, A., Okuda, Y. & Nakai, J. (1983). *Appl. Opt.* **22**, 1329–1336.
Pelliciari, C., Spiga, D., Bonnini, E., Buffagni, E., Ferrari, C., Pareschi, G. & Tagliaferri, G. (2015). *Proc. SPIE*, **9603**, 96031P.
Salmaso, B., Spiga, D., Basso, S., Ghigo, M., Giro, E., Pareschi, G., Tagliaferri, G., Vecchi, G., Pelliciari, C., Burwitz, V., Sanchez del Rio, M., Ferrari, C., Zappettini, A., Uslenghi, M., Fiorini, M., Parodi, G., Ferreira, I. & Bavdaz, M. (2018). *Proc. SPIE*, **10699**, 106993I.
Sánchez del Río, M. & Cerrina, F. (1992). *Rev. Sci. Instrum.* **63**, 936–940.
Spiga, D., Pareschi, G., Pelliciari, C., Salmaso, B. & Tagliaferri, G. (2012). *Proc. SPIE*, **8443**, 84435F.
Spiga, D., Pelliciari, C., Bonnini, E., Buffagni, E., Ferrari, C., Pareschi, G. & Tagliaferri, G. (2014). *Proc. SPIE*, **9144**, 91445I.
Spiga, D., Pelliciari, C., Salmaso, B., Arcangeli, L., Bianucci, G., Ferrari, C., Ghigo, M., Pareschi, G., Rossi, M., Tagliaferri, G., Valsecchi, G., Vecchi, G. & Zappettini, A. (2016). *Proc. SPIE*, **9963**, 996304.